Journal of Chromatography B, 871 (2008) 220–226

Contents lists available at ScienceDirect

Journal of Chromatography B

journal homepage: www.elsevier.com/locate/chromb

Phenotype differentiation of three *E. coli* strains by GC-FID and GC–MS based metabolomics☆

Jing Tian[a,b], Chunyun Shi[a,b], Peng Gao[b], Kailong Yuan[b], Dawei Yang[a,b], Xin Lu[b], Guowang Xu[b,*]

[a] Department of Modern Technology, Dalian Polytechnic University, Dalian 116034, China
[b] Key Laboratory of Separation Science for Analytical Chemistry, Dalian Institute of Chemical Physics, Chinese Academy of Sciences, Dalian 116023, China

ARTICLE INFO

Article history:
Received 5 February 2008
Accepted 18 June 2008
Available online 27 June 2008

Keywords:
Metabolomics
E. coli
Phenotype
GC-FID
GC–MS

ABSTRACT

Two mutants of *E. coli* with deletion of *sdhAB* and *ackA-pta* genes respectively and their wild-type strains were subjected to gas chromatography-flame-ionization detection (GC-FID) and gas chromatography-mass spectrometry (GC–MS) metabolomics analysis. Intracellular metabolites of the three strains were profiled by GC-FID firstly. Methodological evaluation of the employed platform indicated that the limit of detection ranges were from 0.2 to 12.5 ng for some representative metabolites and the corresponding recoveries were varied from 68.7 to 122.7%. Secondly, multivariable data analysis was applied to the acquired data sets. As expected, the three phenotypes could be easily differentiated, and the perturbed metabolite pools in the genetically modified strains were screened. Lastly, the metabolites playing key roles in the differentiation were further identified by GC–MS. It was confirmed that succinic acid and aspartic acid were similarly affected in the modified strains. But proline content was altered contrarily. Additionally, deletion of *sdhAB* gene also affected the growth property of relevant mutant greatly. The potential mechanism was postulated accordingly.

1. Introduction

Metabolomics, a science dealing with small molecules, addresses to a combination of data-rich analytical methods together with chemometrics for metabolic profiling and interpreting metabolic fingerprints in complex biological systems. It plays a key role in genetic modified organism assays [1–3]. Owning to the mostly inconspicuous phenotypic changes, it is difficult to correlate genotypes to phenotypes. For instance, about 90% available mutants of the *Arabidopsis* are the silent mutants [4]. Observed realities suggest that a change in the activity of single enzyme—often the result of genetic modification, usually produces a larger signal in the metabolite concentrations than in the metabolic fluxes [5]. So a metabolomics approach is a good option for detecting the modification effects. Raamsdonk et al. [6] proved that *pfk26*Δ, *pfk27*Δ mutants and the wild-type *Saccharomyces cerevisiae* were of the same growth rate, but they exhibited obvious differences in their intracellular metabolite concentrations revealed by metabolomics analysis using ^{1}H-nuclear magnetic resonance (NMR) spectroscopy. According to their results, the content of fructose-6-phosphate was higher in the mutants than in the wild-type, whereas, ATP/ADP showed lower percentages in the mutants.

Metabolomic studies require reliable sensitivity, quantitation data and robustness of analytical methodology. Currently, NMR, gas chromatography-mass spectrometry (GC–MS), capillary electrophoresis-mass spectrometry (CE–MS) and liquid chromatography-mass spectrometry (LC–MS) are the typical techniques prevailing in metabolomics world with varied features [7–10]. GC–MS is a robust and unbiased approach to detecting unexpected changes in transgenic lines [11]. Combined with the easily accessible database of NIST (www.nist.gov), GC–MS gained more application in different fields. Genetically or environmentally modified plant systems have been extensively studied by using GC–MS for many years [12–14]. Prokaryotic cells were also analyzed by GC–MS metabolomics and different data processing strategies were also developed accordingly to extract the implied information contained in the generated data [15,16]. As a well-adopted strategy, gas chromatography-flame-ionization detection (GC-FID) is thought to be more reliable and sensitive for quantitative analysis than GC–MS, whereas, GC–MS can provide more definite qualitative information [17].

Previously, we had constructed two mutants of *E. coli* for the purpose of high succinic acid production. Although the primary fermentation results indicated that the production of succinic acid was

☆ This paper is part of a special volume entitled "Hyphenated Techniques for Global Metabolite Profiling", guest edited by Georgios Theodoridis and Ian D. Wilson.

* Corresponding author at: National Chromatographic R & A Center, Dalian Institute of Chemical Physics, the Chinese Academy of Sciences, 457 Zhongshan Road, Dalian 116023, China. Tel.: +86 411 84379530; fax: +86 411 84379559.
E-mail address: xugw@dicp.ac.cn (G. Xu).

1570-0232/$ – see front matter © 2008 Elsevier B.V. All rights reserved.
doi:10.1016/j.jchromb.2008.06.031

not improved, the genome-wide changes affecting the metabolic activity of the cells were expected to be in effect. Here, we employed GC-FID and GC–MS metabolomics tactics to differentiate the phenotypic changes of the mutant and the wild-type strains. GC-FID was used to collect the metabolic profiling data for multivariate analysis, the significantly changed metabolites were then subjected to identification by GC–MS.

2. Experimental

2.1. Strains and medium

E. coli 1.1566 (wild-type), DC100 (Δ*sdhAB*) and DC101 (Δ*ackA-pta*) were obtained from Group 1816 of Dalian Institute of Chemical Physics, Chinese Academy of Sciences. DC100 was the mutant of deletion of succinodehydrogenase (SDH) gene, and DC101 was the acetate kinase gene knocked out mutant. LB broth was purchased from Chinese Institute of Import & Export Commodity Inspection Technology (Beijing, China). Cell concentrations were determined by monitoring turbidity of the cultures at wavelength of 600 nm (OD600). The turbidity of the culture was then converted to cell dry weight (CDW)/ml. Residual glucose was quantified using Olympus AU 2700 biochemical analyzer (Olympus, Tokyo, Japan) by employing glucose oxidase method.

2.2. Chemicals and instruments

Dimethylformamide (DMF) and *N*,*O*-bis(trimethylsilyl)trifluoroacetamide (BSTFA) were the products of Sigma–Aldrich (Steinheim, Germany). Methanol, chloroform and pentaerythritol were all purchased from TEDIA (Fairfield, OH). The mixed standard stock solution of amino acids was prepared in the distilled water (1 mg/ml), and organic acids were prepared in methanol (Table 1).

Freeze drying system (FREEZONE4.5) was from LABCONCOC (Kansas, MI). GC-FID detection was performed on an Agilent 6890N GC system (Santa Clara, CA). GC–MS analysis was accomplished on a Shimadzu QP 2010 GC–MS system (Kyoto, Japan). Water used in the experiments was purified with Milli-Q system (Bedford, MI).

2.3. Bacterial growing, quenching and extraction

Three *E. coli* strains were cultured in LB broth with constant agitation (160 rpm) aerobically at 30 °C for 12 h. Fresh culture of each was diluted with aseptic broth to the final concentration of 7.5×10^8 colony forming unit/ml using a bioMerieux (France) DENSIMAT transmissometer. 0.5 ml of bacterial suspension for each was added to 50 ml LB broth in shake flask (150 ml) and then cultured with constant agitation (160 rpm) until to exponential growth phase at 30 °C aerobically. Every strain was cultured in parallel for nine bottles, which generated totally 27 samples.

20 ml of bacterial suspension of each strain was centrifuged ($3000 \times g$) at 4 °C for 5 min. The pellet was washed with aseptic physiological saline in triplicate at 4 °C individually. 1 ml of −45 °C methanol was added to each and the mixtures were settled at 4 °C for 10 min. The turbidities of the suspensions were adjusted to the lowest turbidity in the 27 samples using cold methanol for the convenience of easy comparison. Subsequently, 1 ml of −45 °C chloroform, 0.5 ml purified water and 9 μl of 0.6 mg/ml pentaerythritol (internal standard) were added to 1 ml bacterial suspension for each and vortexed for 1 min, respectively. After centrifugation for 5 min at $6000 \times g$, the supernatant was filtered through 0.22 μm organic membrane. The filtrate was lyophilized and stored in a −80 °C refrigerator until further processing.

2.4. Derivatization procedure

Because silylation regents were more effective to react with hydroxyl, carboxyl and hydrosulfide groups, the BSTFA was selected as the derivatization regent. The solvent used was DMF. The ratio of BSTFA to DMF was 1:1 (v/v, totally 150 μl). The derivatization was accomplished at 60 °C for 40 min.

2.5. GC–MS analysis

GC–MS analysis was accomplished on a Shimadzu QP 2010 GC–MS system using a 30 m × 0.25 mm (i.d.) fused-silica capillary column chemically bonded with 0.25 μm DB5-MS stationary phase (J&W Scientific, Folsom, CA). The injectior temperature was 280 °C and split ratio was 10:1. Helium was used as carrier gas with linear velocity of 35.0 cm/s and an equilibration time of 3 min. The column temperature was initially kept at 70 °C for 5 min and then increased to 280 °C at 5 °C/min, held for 5 min. The MS scan parameters included a mass scan range of *m*/*z* 40–600, a scan interval of 0.5 s, a scan speed of 1000 μm/s, and a detector voltage of 0.9 kV. The ion source temperature was set at 200 °C, and the interface temperature was 280 °C. The solvent cut time was 6 min.

2.6. GC-FID analysis

GC-FID analysis was accomplished on an Agilent 6890 GC-FID system. The detector temperature was 300 °C. The other analytic conditions including the column type and column temperature, the injectior temperature, split ratio, carrier gas and the linear velocity were the same as those of GC–MS analysis.

2.7. Data processing

Peaks with signal to noise ratios (S/N) higher than 10 in the GC-FID data set were selected, and their areas were quantitated against the internal standard through dividing corresponding areas by the internal standard area. The processed data were fed to SIMCA-P software (Umea, Sweden) for multivariate data analysis using the algorithm of principal component analysis (PCA). Variables playing key roles in the pattern recognition model were extracted and then identified via GC–MS assay utilizing commercial compounds.

Table 1
Linearity and detection limit of standards

Compounds	Linear range (μg/ml)	*n*	r^2	Limit of detection (ng, on column)
L-Alanine	5–1000	8	0.9979	0.31
L-Leucine	5–1000	8	0.9944	0.56
L-Threonine	5–1000	8	0.9898	3.41
L-Proline	5–1000	8	0.9981	0.37
L-Glutamic acid	10–1000	6	0.9948	12.50
L-Phenylalanine	5–1000	7	0.994	2.50
L-Lysine	5–1000	7	0.9997	2.96
L-Aspartic acid	5–1000	7	0.9997	3.63
Phosphate	1–1000	8	0.9982	0.24
Glycerol	1–1000	8	0.995	0.48
Malate	1–1000	8	0.9998	0.53
Succinate	1–1000	8	0.9954	0.50
Myristic acid	1–1000	8	0.9997	0.84
Palmitic acid	1–1000	8	0.9967	0.37
Stearic aid	5–1000	7	0.9997	1.50

"*n*": number of concentration points across the range.

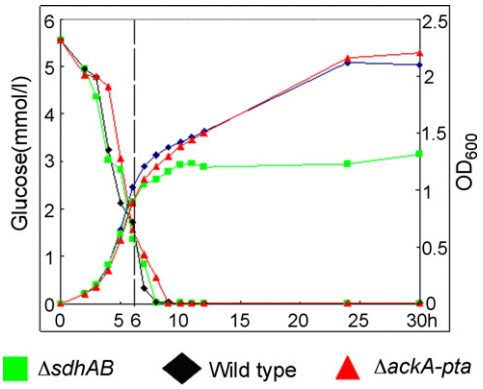

Fig. 1. Growth and the residual glucose curves of the three strains. Dashed line indicated the sampling point at 6 h.

3. Results and discussion

3.1. Growth characteristics of the three strains

Under the aerobic conditions, the growth curves of three strains were investigated. The wild-type and the DC101 shared with the similar growth features (Fig. 1), but the strain of DC100 was characterized of lower yield of biomass, nearly half of the wild-type after 30 h cultivation. The residual glucose concentrations in the fermentation liquid of the three strains changed similarly. This phenomenon indicated that deletion of *sdh* gene severely compromised the growth of *E. coli*. According to Fig. 1, these three strains were all approached to exponential growth phase during the period of 5–8 h, so the sampling time was fixed to the time point of 6 h.

3.2. Analytical characteristics of the GC-FID method developed

In order to evaluate the applicability of the adopted strategy, methodological appraisal of the GC-FID platform was conducted briefly using some commonly found compounds in bacterial cells. The linearity of response was determined by using serial standard solutions ranging from 5 to 1000 μg/ml for amino acids and 1–1000 μg/ml for organic acids and other compounds. Calibration curves for the tested compounds were adjusted using the internal standard. For most of the investigated chemicals, the correlation coefficients of determination (r^2) were generally satisfied (Table 1). Limit of detection was defined as the concentration of a compound resulting in a peak with a signal-to-noise ratio (S/N ratio) higher than 3, corresponding to the range of 0.2–12.5 ng for different individuals (Table 1).

Table 2
Recoveries determined by spiking standards to *E. coli* cell suspension

Compounds	Recoveries (%)	
	Average	R.S.D. (n = 3)
L-Alanine	71.2	5.1
L-Threonine	72.3	5.4
L-Proline	68.7	1.3
L-Aspartic acid	77.4	12.5
Phosphate	122.7	1.7
Malate	79.8	1.2
Succinate	73.4	1.7
Myristic acid	83.6	1.8
Palmitic acid	85.0	1.6

At the same time, the serial standard solutions were used to investigate the reproducibility. After corrected with internal standard, the relative standard deviations (R.S.D.s) of peak areas for the standards of different concentrations were acceptable, the R.S.D. of peak areas varied from 0.7 to 6.2%. To study the extraction recoveries of the metabolites from cellular samples, known amounts of compounds were spiked to cell suspensions of *E. coli* prior to extraction and lyophilization at the concentration of ~15 ng/μl for each. Determined by the quantitation results from the spiked and unspiked samples, the recoveries varied from 68.7 to 122.7% (Table 2). These parameters ensured that the data acquired from GC-FID were acceptable for further analysis. Fig. 2 showed the typical GC-FID chromatograms of intracellular metabolites of the three strains.

3.3. Metabolic fingerprint PCA analysis

GC-FID data were used to compare the phenotypic differences amid the three strains by using PCA. Processed data showed that the three strains could be easily differentiated from each other (Fig. 3). The PCA scores plot and loading plot of the wild-type to Δ*ackA-pta* strains and the wild-type to Δ*sdhAB* strains were shown in Figs. 4 and 5. In the loading plot, the farther the compounds (variables) locate from the origin, the more important they are for the differentiation pattern. These metabolites were taken out for further identification by GC–MS. After *t*-test, it was found that all compounds in Tables 3 and 4 were of p-value ≤ 0.05, showing a significant difference between the wild-type and the genetically modified strains. Obviously, the metabolite pools of succinic acid, proline and aspartic acid were affected in both mutants.

Owning to the advantages of GC–MS and GC-FID individually, combining using these two platforms is more preferable in

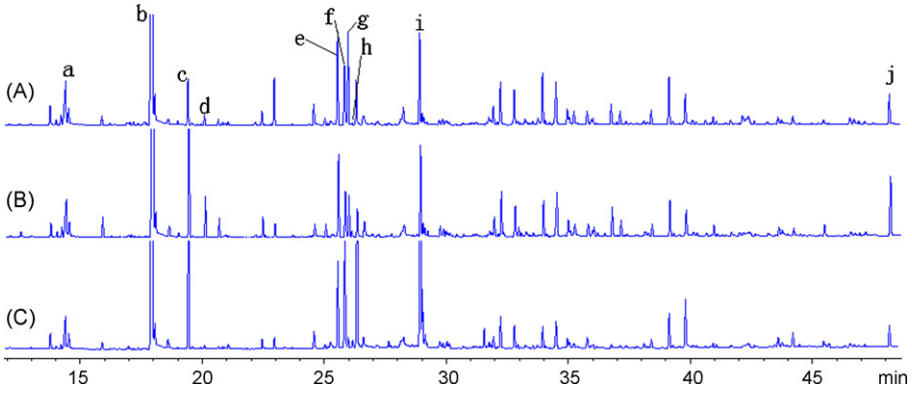

Fig. 2. Intracellular metabolite GC-FID chromatograms of wild-type *E. coli* (A), DC101 (B) and DC100 (C). (a) Lactic acid; (b) phosphoric acid; (c) succinic acid; (d) pyrimidine; (e) pentaerythritol; (f) proline; (g) aspartic acid; (h) phenylalanine; (i) glutamate; (j) uracil (peak identification was confirmed by GC–MS using commercial standards).

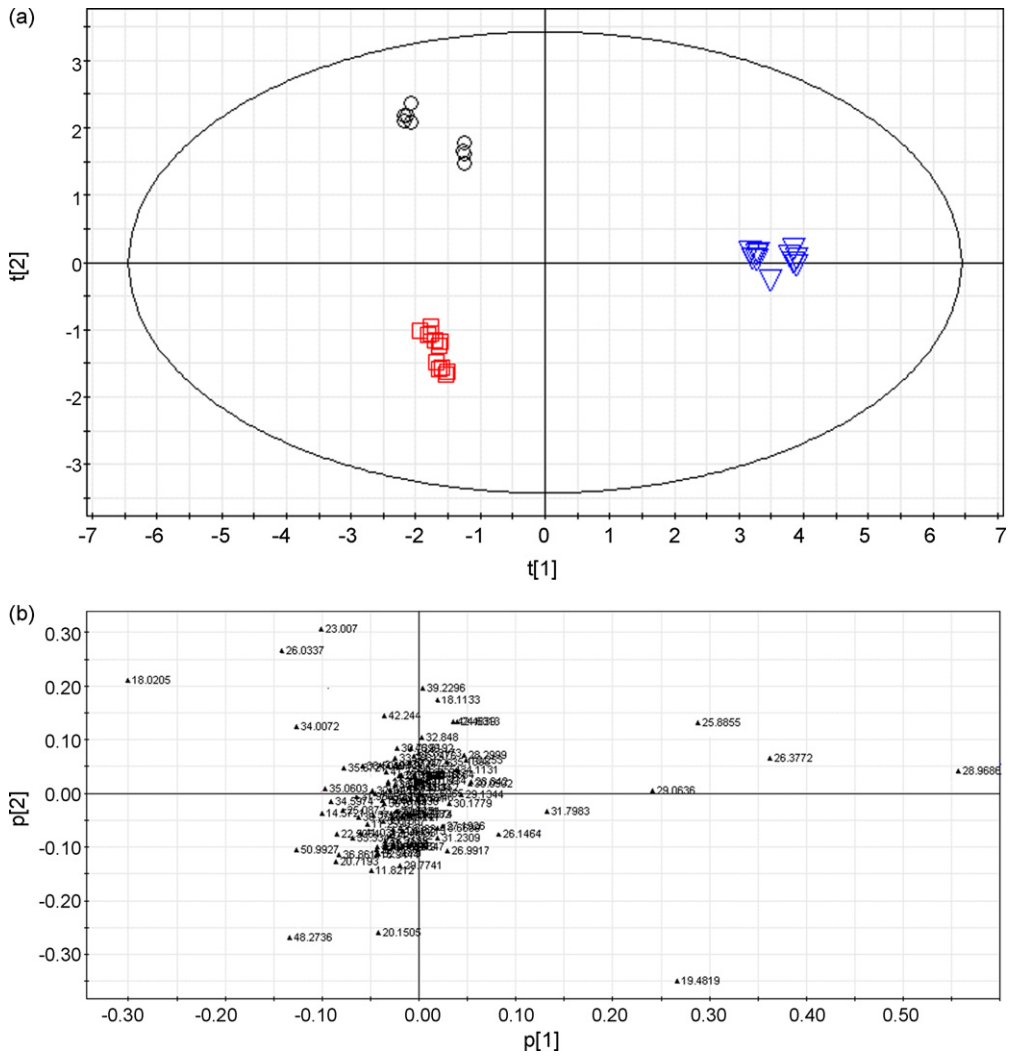

Fig. 3. PCA scores plot (a) and loading plot (b) of the wild-type (○), Δ*ackA-pta* (□) and Δ*sdhAB* (▽) strains based on GC-FID data.

analytical biochemistry. Many types of samples and many endogenous or exogenous compounds had been analyzed by this strategy [18–21]. This could balance the quantitative and qualitative concerns in most circumstance.

It can be anticipated that the concentration of succinic acid would be elevated in the genetic modified strains compared to the wild-type because of the blockage of branch pathways consuming pyruvic acid and succinic acid. The enlargement of intracellular metabolite pool of succinic acid was more significant in DC100 than in DC101 ($p < 0.05$), because the deletion of *sdhAB* might be a substantially direct signal to interrupt the consumption of succinic acid.

Interestingly, the deletion of *sdhAB* gene severely compromised the growth property of *E. coli* compared to the destruction of *ackA-pta* gene. Under the aerobic condition, succinate is only an intermediate of the tricarboxylic acid (TCA) cycle or the glyoxalate shunt metabolism [22]. Destruction of *sdhAB* gene would result in destruction of the integrity of TCA circle and cause the activa-

Table 3
Metabolites with statistical difference in the wild-type and DC101 (Δ*ackA-pta*)

Metabolites		Concentrations (g/g CDW)		*p*
Retention time (min)	Compounds	*E. coli* 1.1566	DC101 (Δ*ackA-pta*)	
11.82	Alanine	–	5.98×10^{-4}	1.94×10^{-6}
18.11	Glycerol	9.24×10^{-4}	6.28×10^{-4}	3.48×10^{-3}
19.48	Succinic acid	6.16×10^{-4}	1.87×10^{-3}	9.18×10^{-10}
20.15	Pyrimidine	1.30×10^{-4}	5.08×10^{-4}	3.64×10^{-19}
25.89	Proline	5.77×10^{-4}	3.82×10^{-4}	3.05×10^{-10}
26.03	Aspartic acid	6.50×10^{-4}	3.04×10^{-4}	2.15×10^{-5}
26.37	Phenylalanine	–	4.30×10^{-5}	1.07×10^{-8}
48.27	Uracil	1.98×10^{-4}	3.97×10^{-4}	5.24×10^{-14}

"–": undetected.

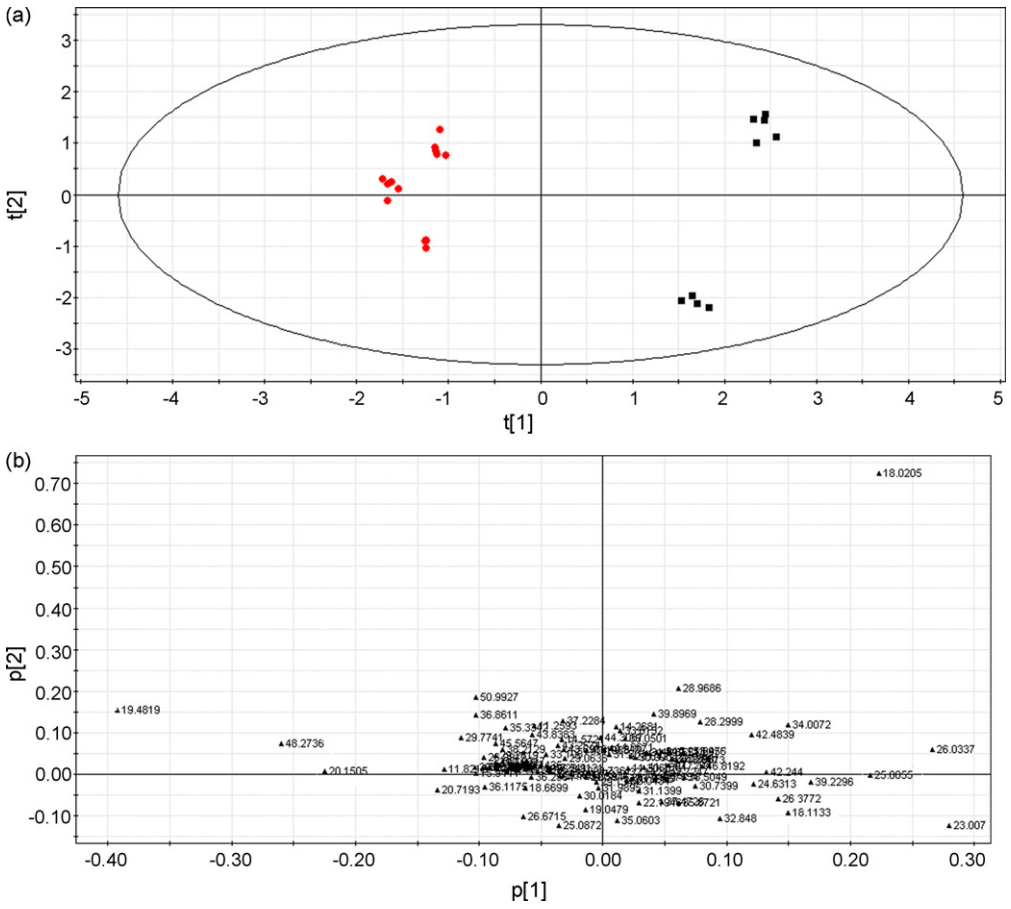

Fig. 4. PCA score plot (a) and loading plot (b) of the wild-type (■) and Δ*ackA-pta* (●) strains based on GC-FID data.

tion of glyoxylate shunt which is usually not active in common circumstances. For 1 mol of succinate generation, the net pyruvate consumption of glyoxylate shunt is two times of TCA circle [23]. Intracellular succinate concentration was found elevated greatly in DC100. The interrupted TCA circle brought about the deficiency of energy generation; the higher content of succinate caused the excessive consumption of pyruvate. Thus, the lower biomass formation was observed in DC100.

Acetate is usually excreted by *E. coli* as an end product and *E. coli* cannot endure higher concentration of acetate in most circumstances. Acetate excretion is controlled by acetate switch. When cultured in glucose medium, the switch is triggered following the onset of stationary phase, at which point the primary carbon source is fully consumed and acetate will be assimilated as carbon source [24]. So destruction of acetate production might not severely affect the growth of *E. coli*. Despite the accumulation of intracellular succinate, we were not able to observe signs of its over-production in the fermentation liquid. So it could be postulated that metabolism of succinate and the relevant metabolites was under stringent regulation in *E. coli*. Furthermore, in *E. coli* cell, succinate dehydrogenase broadly interacted with other enzymes taking part in DNA replication (e.g. DNA polymerase II), protein synthesis (e.g. 30S ribosomal protein S2 and tyrosyl-tRNA synthetase), lipid metabolism (e.g. long-chain-fatty-acid–CoA ligase) and transcriptional regulators (e.g. transcriptional regulatory protein rtcR), etc. (www.ecocyc.org) compared to *ackA-pta* gene product. So we could conclude that SDH

Table 4
Metabolites with statistical difference in the wild-type and DC100 (Δ*sdhAB*)

Metabolites		Concentrations (g/g CDW)		*p*
Retention time (min)	Compounds	*E. coli* 1.1566	DC100 (Δ*sdhAB*)	
18.02	Phosphoric acid	1.03×10^{-3}	8.42×10^{-4}	5.00×10^{-3}
19.48	Succinic acid	6.16×10^{-4}	2.39×10^{-3}	8.39×10^{-13}
20.15	Pyrimidine	1.30×10^{-4}	2.72×10^{-4}	3.29×10^{-7}
25.89	Proline	5.77×10^{-4}	1.08×10^{-3}	7.95×10^{-12}
26.03	Aspartic acid	6.50×10^{-4}	1.03×10^{-4}	2.46×10^{-6}
26.37	Phenylalanine	–	5.25×10^{-5}	6.44×10^{-10}
28.97	Glutamic acid	4.45×10^{-4}	1.61×10^{-3}	3.76×10^{-14}
35.06	Cadaverine	8.00×10^{-5}	3.83×10^{-5}	3.45×10^{-6}
48.27	Uracil	1.98×10^{-4}	1.46×10^{-4}	2.59×10^{-6}

"–": undetected.

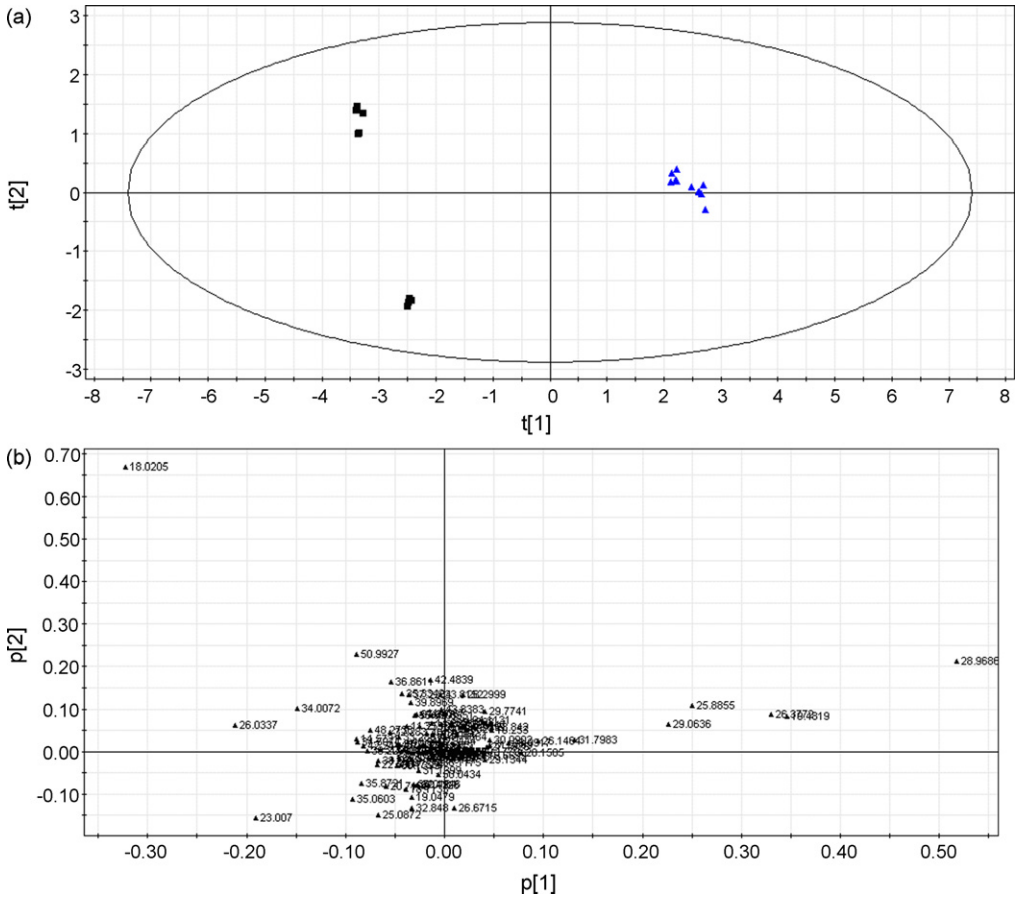

Fig. 5. PCA score plot (a) and loading plot (b) of the wild-type (■) and Δ*sdhAB* (▲) strains based on GC-FID data.

also played a crucial role in keeping the biological stabilization of *E. coli*.

4. Conclusions

In conclusion, the recently introduced functional genomics technology, especially metabolomics, is revolutionizing research in the biological sciences. Although still in its infancy, metabolomics is a convenient tool to understand bacterial functioning in microbiology. Using GC-FID and GC–MS platform, the phenotypic difference among three strains of *E. coli* could be easily discerned. Deletion of *sdhAB* gene brought about a much more complex perturbation on *E. coli* cell than deletion of *ackA-pta* gene. The most profound effect stemming from deletion of *sdhAB* gene might be the perturbation on broad interactions amid the cellular components and, potentially, the involved metabolic pathways. This research work proved again that metabolomics analysis is indeed a good approach for phenotype differentiation.

Acknowledgments

The studies have been supported by National Basic Research Program (2003CB716003, 2004CB719605 and 2007CB707800) of State Ministry of Science and Technology of China, the National Natural Science Foundation of China (no. 20776029) and the Knowledge Innovation Program of the Chinese Academy of Sciences (K2006A8, K2006A13).

References

[1] I. Wilson, Mol. Syst. Biol. 3 (2007) 113.
[2] D. Hwang, J.J. Smith, D.M. Leslie, A.D. Weston, A.G. Rust, S. Ramsey, P. de Atauri, A.F. Siegel, H. Bolouri, J.D. Aitchison, L. Hood, Proc. Natl. Acad. Sci. U.S.A. 102 (2005) 17302.
[3] S. Draghici, P. Khatri, A.L. Tarca, K. Amin, A. Done, C. Voichita, C. Georgescu, R. Romero, Genome Res. 17 (2007) 1537.
[4] R.D. King, K.E. Whelan, F.M. Jones, P.G. Reiser, C.H. Bryant, S.H. Muggleton, D.B. Kell, S.G. Oliver, Nature 427 (2004) 247.
[5] D.A. Fell, J. Exp. Bot. 56 (2005) 267.
[6] L.M. Raamsdonk, B. Teusink, D. Broadhurst, N. Zhang, A. Hayes, M.C. Walsh, J.A. Berden, K.M. Brindle, D.B. Kell, J.J. Rowland, H.V. Westerhoff, K. van Dam, S.G. Oliver, Nat. Biotechnol. 19 (2001) 45.
[7] M.M. Koek, B. Muilwijk, M.J. van der Werf, T. Hankemeier, Anal. Chem. 78 (2006) 1272.
[8] W.B. Dunn, D.I. Ellis, Trends Anal. Chem. 24 (2005) 285.
[9] J. van der Greef, P. Stroobant, R. van der Heijden, Curr. Opin. Chem. Biol. 8 (2004) 559.
[10] O. Fiehn, W. Weckwerth, Eur. J. Biochem. 270 (2003) 579.
[11] U. Roessner, C. Wagner, J. Kopka, R.N. Trethewey, L. Willmitzer, Plant J. 23 (2000) 131.
[12] W. Weckwerth, M.E. Loureiro, K. Wenzel, O. Fiehn, Proc. Natl. Acad. Sci. U.S.A. 101 (2004) 7809.
[13] O. Fiehn, J. Kopka, P. Dormann, T. Altmann, R.N. Trethewey, L. Willmitzer, Nat. Biotechnol. 18 (2000) 1157.
[14] U. Roessner, A. Luedemann, D. Brust, O. Fiehn, T. Linke, L. Willmitzer, A. Fernie, Plant Cell 13 (2001) 11.
[15] N. Ishii, K. Nakahigashi, T. Baba, M. Robert, T. Soga, A. Kanai, T. Hirasawa, M. Naba, K. Hirai, A. Hoque, P.Y. Ho, Y. Kakazu, K. Sugawara, S. Igarashi, S. Harada, T. Masuda, N. Sugiyama, T. Togashi, M. Hasegawa, Y. Takai, K. Yugi, K. Arakawa, N. Iwata, Y. Toya, Y. Nakayama, T. Nishioka, K. Shimizu, H. Mori, M. Tomita, Science 316 (2007) 593.
[16] H.H. Kanani, M.I. Klapa, Metab. Eng. 9 (2007) 39.
[17] M. Ligor, B. Buszewski, J. Sep. Sci. 31 (2008) 364.
[18] N.L. Koryagina, E.I. Savelieva, N.S. Khlebnikova, N.V. Goncharov, R.O. Jenkins, A.S. Radilov, Anal. Bioanal. Chem. 386 (2006) 1395.

[19] M.V. Russo, L. Di, V.P. Avino, Ann. Chim. 94 (2004) 741.
[20] M.A. LeBeau, M.A. Montgomery, M.L. Miller, S.G. Burmeister, J. Anal. Toxicol. 24 (2000) 421.
[21] M.A. Martinez, S. Ballesteros, T.C. Sanchez de la, A. Sanchiz, E. Almarza, A. Garcia-Aguilera, J. Anal. Toxicol. 28 (2004) 609.
[22] M.J. Van der Werf, M.V. Guettler, M.K. Jain, J.G. Zeikus, Arch. Microbiol. 167 (1997) 332.
[23] G.N. Vemuri, M.A. Eiteman, E. Altman, Appl. Environ. Microbiol. 68 (2002) 1715.
[24] M. EI-Mansi, A.J. Cozzone, J. Schiloach, B.J. Eikmanns, Curr. Opin. Microbiol. 9 (2006) 173.